Spatio-Temporal Analysis of Convective Cloud Properties Deriving from Weather Radar Reflectivity during the Decaying Stage of Tropical Storm over the Lower Northern Thailand

Mahavik, N.[1] and Tantanee, S.[2,3]
[1]Department of Natural Resources and Environment, Faculty of Agriculture Natural Resources and Environment, Naresuan University, Phitsanulok, 65000, Thailand, E-mail: nattaponm@nu.ac.th
[2]Department of Civil Engineering, Faculty of Engineering, Naresuan University, Phitsanulok, 65000, Thailand
[3]Centre of Excellence on Energy Technology and Environment, Naresuan University, Phitsanulok, 65000, Thailand

Abstract
Disaster Management is one of the most important responsibilities of the governments all over the world. The systems of disaster prevention, preparedness and mitigation have been well established only in developed countries. For the developing countries including Thailand, people still have suffered from disaster since they are lacking of adequate information to cope with disaster. The weather radar is one of the tools that can provide spatio-temporal information for Nowcast which is useful for hydro-meteorological disasters warning and mitigation system. The extremes of precipitation are usually detected by convective cloud where the updrafts and downdrafts have been strengthened in vertical wind motions These extremes are the vital threat to people during wet season over Thailand. In this study, therefore, we have developed algorithm to extract convective cloud information that is necessary for prediction of precipitation extremes. The algorithm is constructed in Python script using OpenCV library to extract the radar reflectivity of the 1st Plan Position Indicator of radar image. The reflectivity data with the measurement frequency of once per hour has been obtained from the website of Thaiwater.net of which original data provided by Thai Meteorological Department (TMD). This study has been done by using reflectivity data from Phitsanulok radar station which locates in Lower Northern Thailand. The convective cloud regions have been detected by the developed algorithm. In addition, the fitting ellipses (Fitzgibbon and Fisher, 1995) have been applied to derive the properties of convective clouds during Sonca tropical storm in July of 2017. Results show that the number of convective cloud regions has abruptly increased during Sonca period compared to before the storm passing. The average number of convective cloud region has shown clearly of peak time at 17 LST. However, several peaks of total area on the convective region at hourly scale have also been found. The spatio-temporal analysis of the extracted storm information demonstrates the severe pattern of the high frequency convective storm during Sonca event over windward slope. The number of convective storm doubled increases comparing with period prior to Sonca storm.

1. Introduction

Flash flood and landslide are mainly triggered by exceeding rainfall amount above the maximum capacity of soil resistance over the risky areas. Analysis of mesoscale precipitation areas is considerable meteorological significance because the features of subsynoptic-scale air motions including convective and stratiform regions of cloud will improve our understanding on mechanism of larger and smaller scales of the atmosphere (Austin and Houze, 1970). Mesoscale Convective Systems (MCSs) are the largest convective storms which are taken into account for a large proportion of precipitation in both the tropics and warmer latitudes (Houze, 2004). There are many factors of MCSs that produce contiguous precipitation area of about100 km. Many studies have investigated MCSs contribution to extreme rainfall implying disaster related to their events over the world (e.g. Rigo and Llasat 2004, Rigo and Llasat 2005, Schumacher and Johnson, 2006, Rigo and Llasat, 2007, Carbone and Tuttle, 2008 and He et al., 2016). Schumacher and Johnson (2006) had studied extreme rain events during 1999-2003 in U.S. They used National composite radar reflectivity to classify each event as the MCSs, Synoptic, or the tropical system and then to the sub-classifications based on their organizational structures. They found 74% of warm-season events are associated with MCSs producing their peak rainfall time between 2100 and 2300 Local Standard Time (LST).

Radar reflectivity has been widely used to study characteristics of MCSs due to its advantages on spatial and temporal resolution (e.g. Rigo and Llasat, 2004, Schumacher and Johnson, 2006, Rigo and Llasat, 2007, Lang et al., 2007, He et al., 2016 and Satomura et al., 2011). The storm morphology has been detected by employing an ellipse-fitting technique of which the major and minor axes lengths are extracted from the geometry of the fitted ellipses (Lang et al., 2007). In addition, to improve convective parameterizations, the ellipse-fitting technique is also applied to radar sensor on satellite of the Tropical Rainfall Measuring Mission (TRMM) Precipitation Radar (PR) or TRMM/PR to detect the storm morphology and rainfall characteristics (Nesbitt et al., 2006). Finding the contribution of storm morphology characteristics in land and ocean will provide more understanding on the importance of rainfall modes difference regionally. Using radar sensor on satellite board, MCSs are found that they are the cause of rainfall over selected land regions up to 90%. In tropics-wide extent, MCSs are responsible for more than 50% of rainfall in almost all regions with average annual rainfall exceeding 3 mm day^{-1}.

Risky areas during tropical storm events over the Indochina have been regularly affected during the boreal summer. In the latter half of July 2017, tropical storm named Sonca coming from South China Sea had affected to northern and northeastern regions of Thailand when it was dissipating to tropical depression (Bangkok Post, 2017). Phitsanulok province located in the Lower Northern Thailand had also been affected which caused large area of paddy field inundation and the severe flashflood attacked more than 50 houses over the upper part of the province. However, there is no research about the situation of MCSs during the Sonca over the Lower Northern Thailand. Satomura et al., (2013) proposed the radar echo composite map using multiple weather radars crossing the nation boundaries over the Indochina during Typhoon Lekima in October 2007 to understand typhoon structures of tropical disturbance. Compared with the radar echo composite map, mesoscale numerical model simulation reproduced the typhoon center position very well, and it also caught the characteristics of internal structure of decaying typhoon in the Indochina. Nevertheless, the spatio-temporal analysis of decaying tropical storm is not yet well described using the high-resolution data.

Therefore, the objectives of this study are; to detect the convective cloud regions by extracting the radar data over Phitsanulok province, to spatio-temporal analyze during the storm event in July 2017, and to describe the implemented methodology of the radar image data process. In the developing countries including Thailand, official mosaicked radar products are unavailable to be used for research purpose and real-time monitoring of severe weather. Thus, this study uses free-online radar data providing as images that have been observed at Phitsanulok radar, in the middle Thailand.

2. Data and Study areas

Radar reflectivity data used in this study has been observed by Phitsanulok weather radar station. The radar site is located in the Lower Northern Thailand (Figure 1) at the geographic coordinates at latitude of 16°46'30.358"N and longitude of 100°13'4.312"E on the height of the terrain at 47 m above mean sea level with tower height of 30 m. The radar data is observed by Thai Meteorological Department (TMD) at four time per hour, While the data has been archived as images by Hydro and Agro Informatics Institute (HAII) at frequency of once per hour in format of GIF. The active radius of the Phitsanulok radar is 240 km observing in C-band frequency with beam width at 1°. In this study, the Plan Position Indicator (PPI) images of the first elevation at 0.5° from horizontal line have been collected and used in the analysis.

The topography of radar coverage area varies from flood plain in the central and southern part to mountainous area in the surrounding of the western, northern and eastern part. Over the radar coverage area, there are also the important river tributaries of Chao Phraya river basin which are Ping, Yom and Nan river basin. During southwesterly monsoon season, the rainfall abruptly increases over the Indochina region ranging from May to the mid of October. The amount of rainfall over this region is under the influences of the convergence of prevailing wind that brings the moisture to the low depression at the location of Intertropical Convergence Zone. In addition, the tropical disturbances from north western Pacific Ocean usually bring a large amount of rainfall in terms of tropical depression. In this study, radar data during influencing period of Sonca tropical storm during 24 to 29 July 2017 according to TMD warning announcement has been processed and analyzed.

3. Methodology

3.1 Extraction of Radar Reflectivity

The radar images provided by TMD are shown in color ranges superimposed over terrain as its background. The color ranges indicate intensity of radar reflectivity in ascending order of rainfall intensity of green (slight rain), yellow to oranges (medium rain), and red to white (heavy rain). The images cannot be instantly processed or analyzed in digital image processing (DIP) because it is needed pre-process to transform image to digital information. Therefore, the implemented methodology of radar reflectivity extraction from radar images shown in Figure 2 has been developed using Python script as shown the workflow in Figure 3. First, the image has been cropped to select only radar coverage area. Then, radar reflectivity shown in Figure 2a has been extracted following the pre-defined color ranges as shown in Figure 2b. The threshold method to classify convective storm using radar reflectivity has been used in many studies (e.g. Steiner et al., 1995, Rigo and Llasat 2004 and 2007).

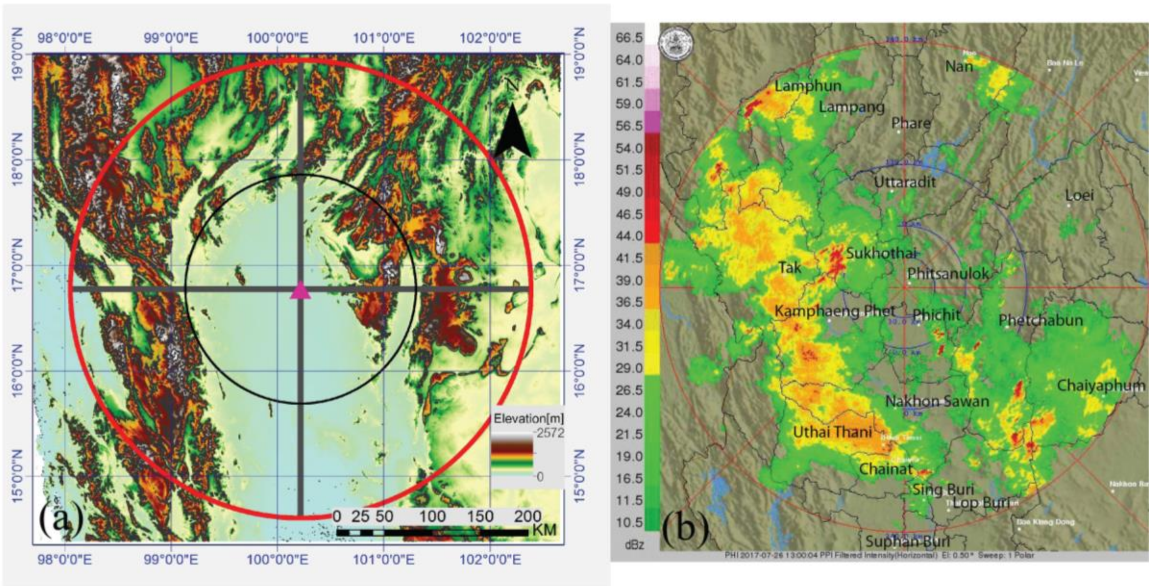

Figure 1: Study area over Phitsanulok, the middle of Thailand (a) active radius of Phitsanulok with two observation ranges at 120 and 240 km (b) radar image of 1st PPI at elevation angle of 0.5° on on 26 July 2017 at 20.25 LST provided by Thai Meteorological department

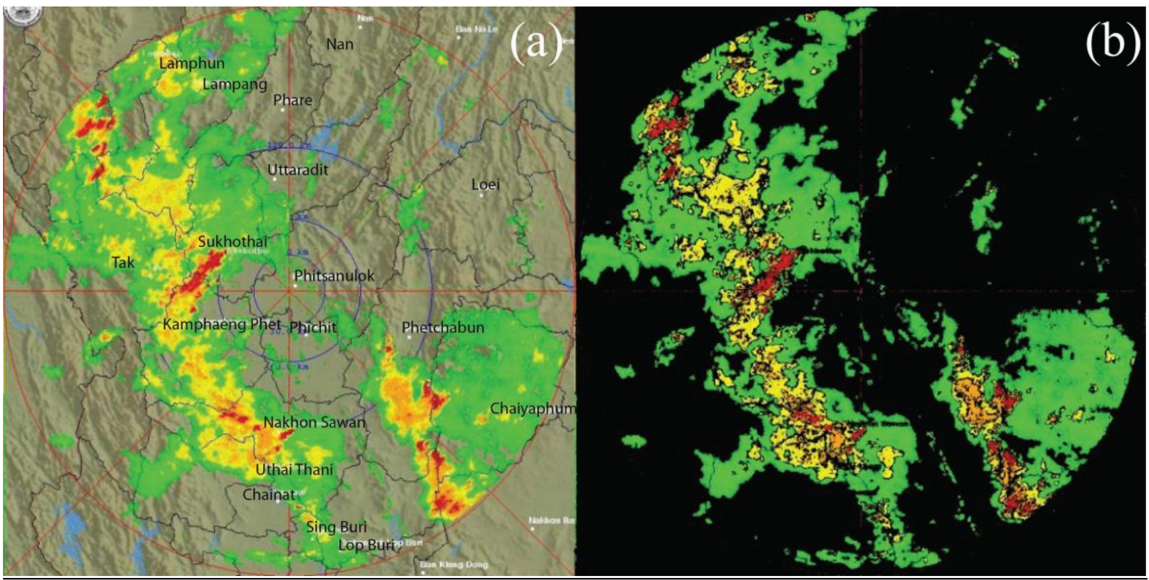

Figure 2: Radar extraction result (a) radar reflectivity with permanent flare to the west of the radar station (b) the extracted radar reflectivity on 26 July 2017 at 13.25 LST

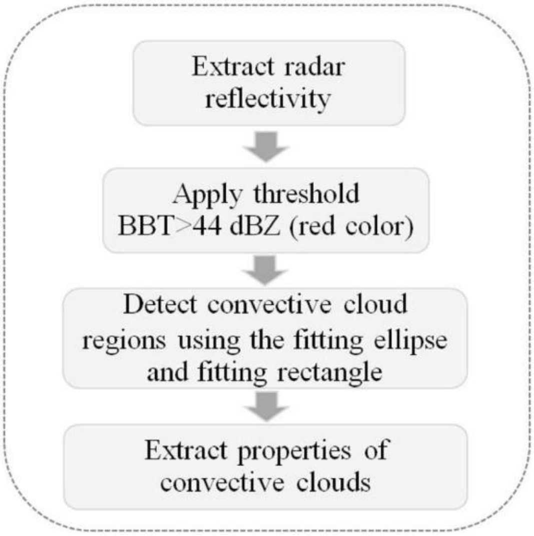

Figure 3: workflow of detection convective cloud properties

Using the raw radar reflectivity, the partition of cloud precipitation can be classified using the 2 and 3 dimensional information of radar scanning (Steiner et al., 1995 and Biggerstaff and Listemaa, 2000). However, without the raw data, the present study simply classifies the convective storm using the extracted radar information from TMD radar images by background-exceedence technique (BET) to identify the core of the convective precipitation (Austin and Houze, 1972 and Houze, 1973). The convective storm has been simply defined the threshold according to the red color ranges at the reflectivity greater than 44 dBZ. The next step is to use the obtained radar reflectivity in the process of radar flares removing.

3.2 Detection of Convective Cloud Properties

In the case of convective cloud detection, we have developed a method to detect convective cloud regions in the hourly radar images using Digital Image Processing (DIP) technique in computer vision field by employing OpenCV-Python library V.3.4.1.15. The morphological transformations have been applied to those extracted reflectivity to detect the convective region. At the beginning, the extracted reflectivity has been converted to grey scale image to be ready to apply kernel convolution of close morphology at size of 15x15 window which is derived from several trials to produce an appropriate result of the processed reflectivity. The morphological close is used to eliminate small holes inside foreground objects following with application of erosion morphology to separate each possible flare apart from the group of rain pixels. Later, edge detection using Canny operator has been firstly applied to detect unwanted line appeared on the reflectivity and, the feature extraction technique of Hough transform (Duda and Hart, 1972), then, was applied to detect those lines from the results of canny application. In order to apply the process of convective cloud detection, the eroded image in greyscale has been searched through for delineating the contour of the pixel objects. The contoured image is used as the main input in the next process. The fitting ellipse (Fitzgibbon and Fisher, 1995) and the fitting rectangle have been applied the extracted possible regions as contour lines. The results of detected convective regions by the fitting ellipse provide convective cloud properties such as major ellipse axis, the ratio between minor and major ellipse axis lengths or AR as shown in Figure 4, as well as the center of convective cloud region from the fitted ellipse.

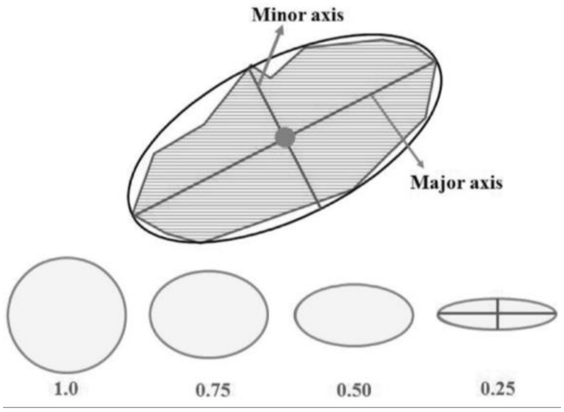

Figure 4: schematic of the fitting ellipse shown in the biggest ellipse envelopes of the convective region in blue region. The axis ratio (AR), the ratio between minor and major fitting ellipse length, is shown as a number

To avoid confusion between radar flares and convective clouds, the criteria of automate convective cloud detection has been set by using the AR exceeding 0.1, the length of major fitting ellipse axis must be in range of 5-480 km and area of the fitting rectangle is greater than 10 sq.km. MCSs are the regions of both convective and stratiform precipitation (Houze, 2004). Steiner et al., (1995) detected radar echo images with convective cloud at horizontal radius of 11 km. However, in this study, to assure the convective detection, we strictly apply both the major of the fitting ellipse and convective size compared to previous study. The results of detected convective cloud regions are shown in Figure 5. The next step is to use the results of detected convective cloud to analyze spatio-temporal variability for searching dominant spatio-temporal pattern over the Sonca storm period.

3.3 Terrain Effect on Radar Beam Observation

To discuss about the terrain effect on propagating radar beam, the simulated beam propagation is needed to reconstruct in the analysis with the terrain. To reconstruct of the propagating radar beam through the atmosphere, the spherical coordinate radar reflectivity was considered with the elevation above mean sea level (MSL) which obtained from the SRTM Digital Elevation Model (DEM) V4 with resolution of 3 arc second (Rabus et al., 2003) for each range bin at resolution of 1 km. The height of each range bin (*H*) was calculated using the standard refraction relation from Rinehart (1999):

$$H = \sqrt{r^2 + R'^2 + 2rR' \sin \emptyset} - R' + H_0$$

Equation 1

where r is the range from the radar to the point of interest, ø is the elevation angle of the radar beam, H_0 is the height of the radar antenna, $R' = 4/3R$, and R is the earth's radius (approximately 6374 km).

4. Results

4.1 Radar Reflectivity Extraction

The reflectivity from 1st Plan Position Indicator (PPI) of the original image is successfully extracted using the predefined color ranges as shown in Figure 2. The radar reflectivity in red color is better delineated and extracted comparing with the original image because among the color ranges the red color is easiest to be defined. The extracted radar reflectivity in the red color ranges will be used as the input for the delineated convective cloud in this study. However, the radar extraction from the simply implementation will be the new path way of radar meteorology in 2-Dimension analysis in the middle of Indochina peninsula due to lacking of raw digital radar data provided for the research community. Although, the extracted reflectivity derived from PPI may be either overshooting or undershooting the convective cloud at some distances, the PPI data is also useful to monitor the severity of storm for developing countries such Thailand. We also realized that the results of using PPI are not be consistent with using Constant altitude plan position indicator (CAPPI) from previous studies of Satomura et al., (2011) and Mahavik et al., (2014). PPI uses information from single elevation to observe the cloud which may subject to precipitating clouds in the far range. In contrast, the CAPPI uses information from several angles during the interpolation processing in the Cartesian grid system using weighting techniques to mitigate either underestimate or overestimate precipitating cloud.

4.2 Detection of Convective Clouds

Convective clouds have been well extracted compared with the original image as shown in Figure 5. Since the beam width is 1°, the far range of radar observation has been increased their horizontal resolution larger than 5 km. Therefore, it is assured that the small convective cloud can be detected within the limitation of minimum convective area at greater than 10 km^2. In the future, the minimum size of convective cloud should be adjusted when the higher resolution of radar observation is in operation. Moreover, with the higher resolution of radar, the suddenly severe storm in smaller size over wider area can be detected, as well.

4.3 Terrain effect on Radar Beam Observation

The terrain effect of radar beam on cloud observation is needed to be discussed to evaluate the quality of the observation. The Wradlib library V.0.9.0 (Heistermann et al., 2013) is used in the analysis using with Python script. The terrain used in beam blockage analysis shows variation in altitude (Figure 6). The east side of Phtisanulok radar occupies rugged terrain with high elevation that obstructs the broadening beam over 50% of beam width. Using the beam-blockage fraction (BBF), the areas of blocked beam by terrain mainly locate in the east side of the radar. The blocked beam areas indicate the reliability of the returned radar power to estimate group of precipitation. The higher BBF represents the higher uncertainty of precipitation estimation over the area. As shown in Figure 6, we simply define the BBF at 50%. The cross section of propagating beam trough atmosphere by considering 1° of beam width according to equation 1 has shown the center of beam obstructed by the mountain range name Phetchabun range in the part of Phitsanulok province (Figure 6c). However, the blocked area is not large in this study and the results of the detected convective clouds are not affected. The suggestion from the beam blockage analysis is that TMD should consider using multiple elevation angles for the analysis and making a radar composite map by mosaicking nearby radar for warning the severe storm that may trigger disaster over the rugged terrain areas.

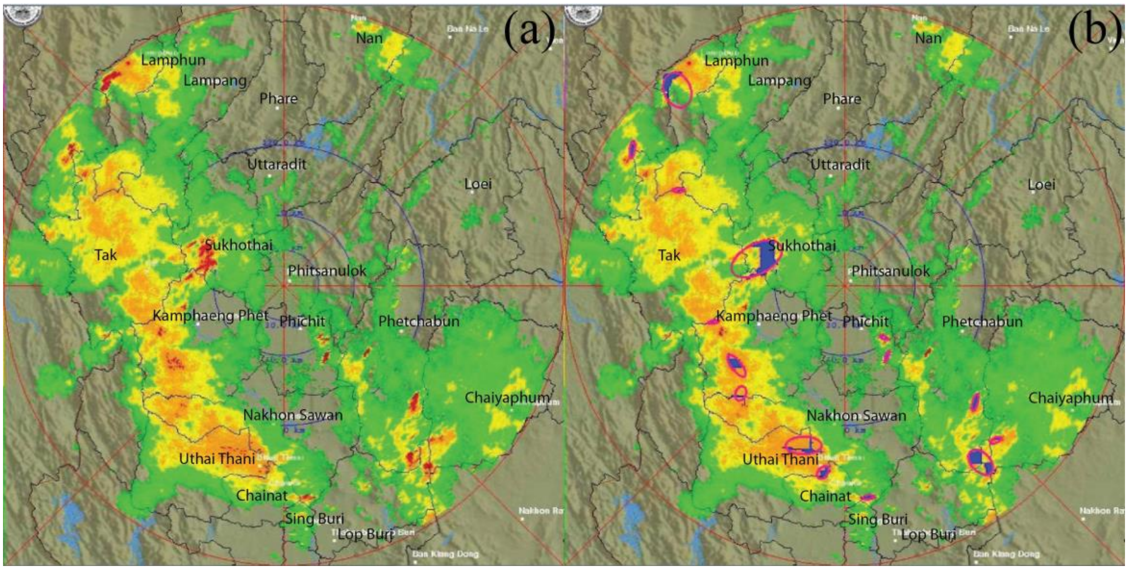

Figure 5: The detected convective storms on 26 July 2017 at 20.25 LST (a) original 1st PPI radar reflectivity (b) detected convective storms superimposed by the fitting ellipse in purple colors

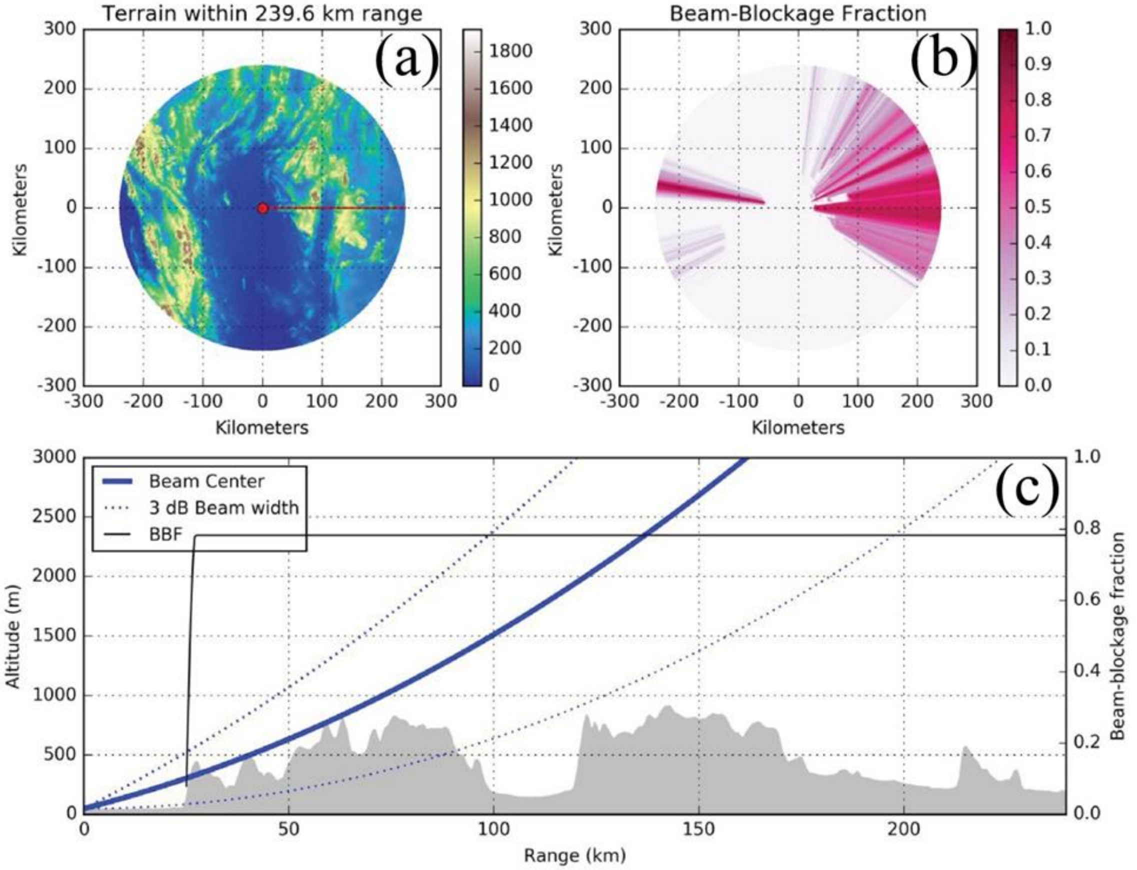

Figure 6: simulation of beam-blockage fraction using beam propagation equation implemented in Wradlib library over the terrain surrounding Phitsanulok radar using elevation angle at 0.5 deg. (a) terrain over the observed area and pointing azimuth direction shown in red line (b) beam-blockage fraction of each radar observation range (c) simulated result of propagating beam at azimuth of 90°

Table1: summary of convective cloud statistics comparing between during Sonca and before Sonca periods

	Properties	Sonca period	Before Soca period
1	Total area (km^2)	50,810.23	31,973.57
2	Average area (km^2)	102.65	91.88
3	S.D. area (km^2)	151.19	120.34
4	Total number of CV	2,651.00	1,112.00
5	Average number of CV	5.36	3.20
6	S.D. number of CV	4.35	2.26
7	Total length of CV (km)	6,754.69	4,737.52
8	Average length of CV (km)	13.65	13.61
9	S.D. length of CV (km)	12.55	11.11

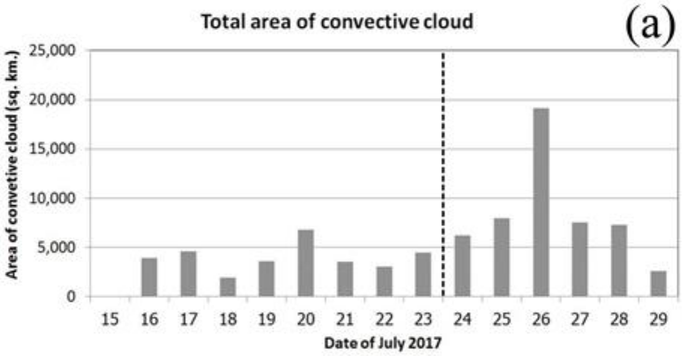

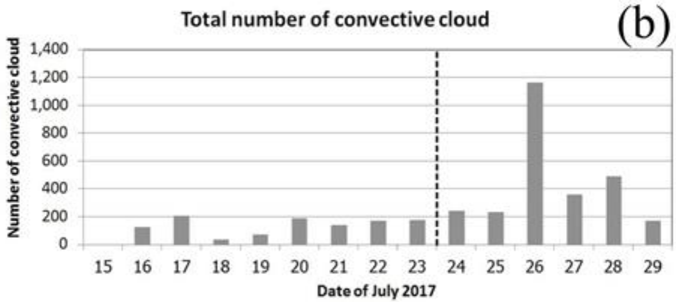

Figure 7: daily statistics of convective clouds (a) total area of convective cloud (b) total number of convective cloud. Dash lines separate during Sonca and before Sonca periods

4.4 Spatio-Temporal Analysis of Convective Cloud Occurrence

Spatio-temporal analysis of convective cloud occurrence will improve the understanding in severity impact of the Sonca over the middle Thailand. As shown in Table 1, comparison of period before and during Sonca event has shown severity in various parameters. The before Sonca period which accounted for 9 days from 15 to 23 July, has shown the small area of convective cloud coverage almost half of the coverage during Sonca period of 6 days from 24 to 29 July. The average lengths of convective cloud for both periods are not different, while the total number of convective cloud during Sonca is larger than double of before the storm period. Total area and number of convective cloud during Sonca are greater than the before storm period especially on 26 July as shown in Figure 7a and 7b.

Average number of convective cloud during Sonca has been analyzed to find the severe hour as diurnal variation. The maximum of average number of the convective cloud at 10 UTC (17 LST) has been found as shown in Figure 8a. However, area average of diurnal variation convective peak has shown the highest peak at 23UTC as shown in Figure 8b. The quasi-stationary convective systems as well as speed and direction of convective storms during Sonca have not been considered in this study. Therefore, the characteristics of storm movement will be further investigated in the future study to classify the severity of the storm.

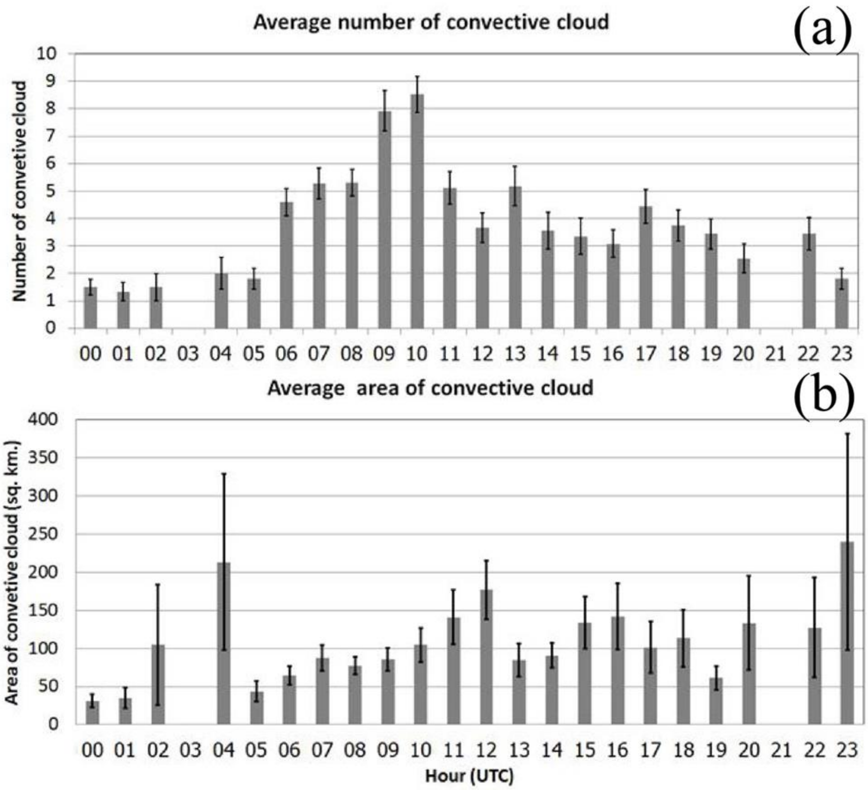

Figure 8: the diurnal variation of convective cloud (a) average number of convective clouds (b) average area of convective clouds. Standard error is shown as error bars

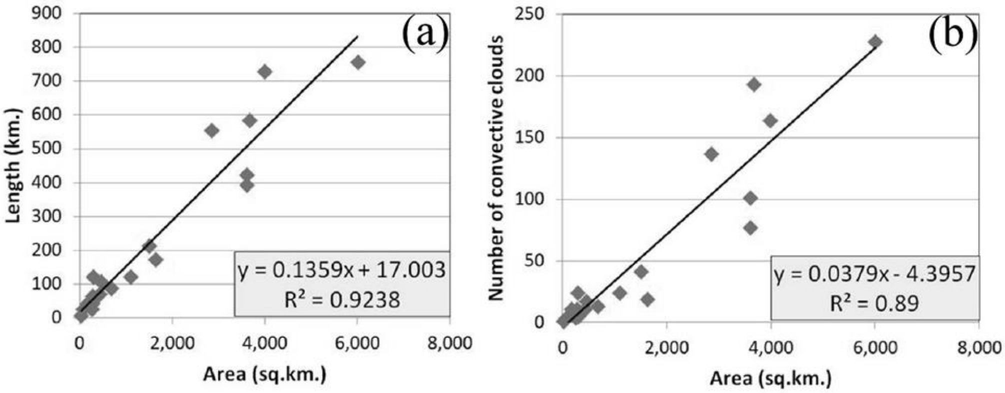

Figure 9: the relation of total area of hourly convective cloud with (a) total of hourly length (b) total number of convective clouds

The total area of hourly convective storm has been analyzed during the Sonca period to find relationship with the extracted convective cloud properties. These properties are total length and total number of which the relationships are as shown in Figure 9. Figure 9(a) shows the strong relationship between the total area and the total length of the convective strong which can summarize that during decaying stage of Sonca storm over the study area, the morphology of strong convective clouds has shown the elongate shapes at certain hour. For example at 11 UTC (18 LST), the total area of convective storm has reach over 6000 km^2, associated with the summation of the longest major fitting ellipse axis of over 700 km as shown in Figure 9a. In addition, the total area of convective storm is also well related to the total number of convective clouds as shown in the Figure 9b. This result can be the suggestion for TMD to monitor the decaying severe storm in both space and time in their analysis before announcing disaster warnings to the people in the future.

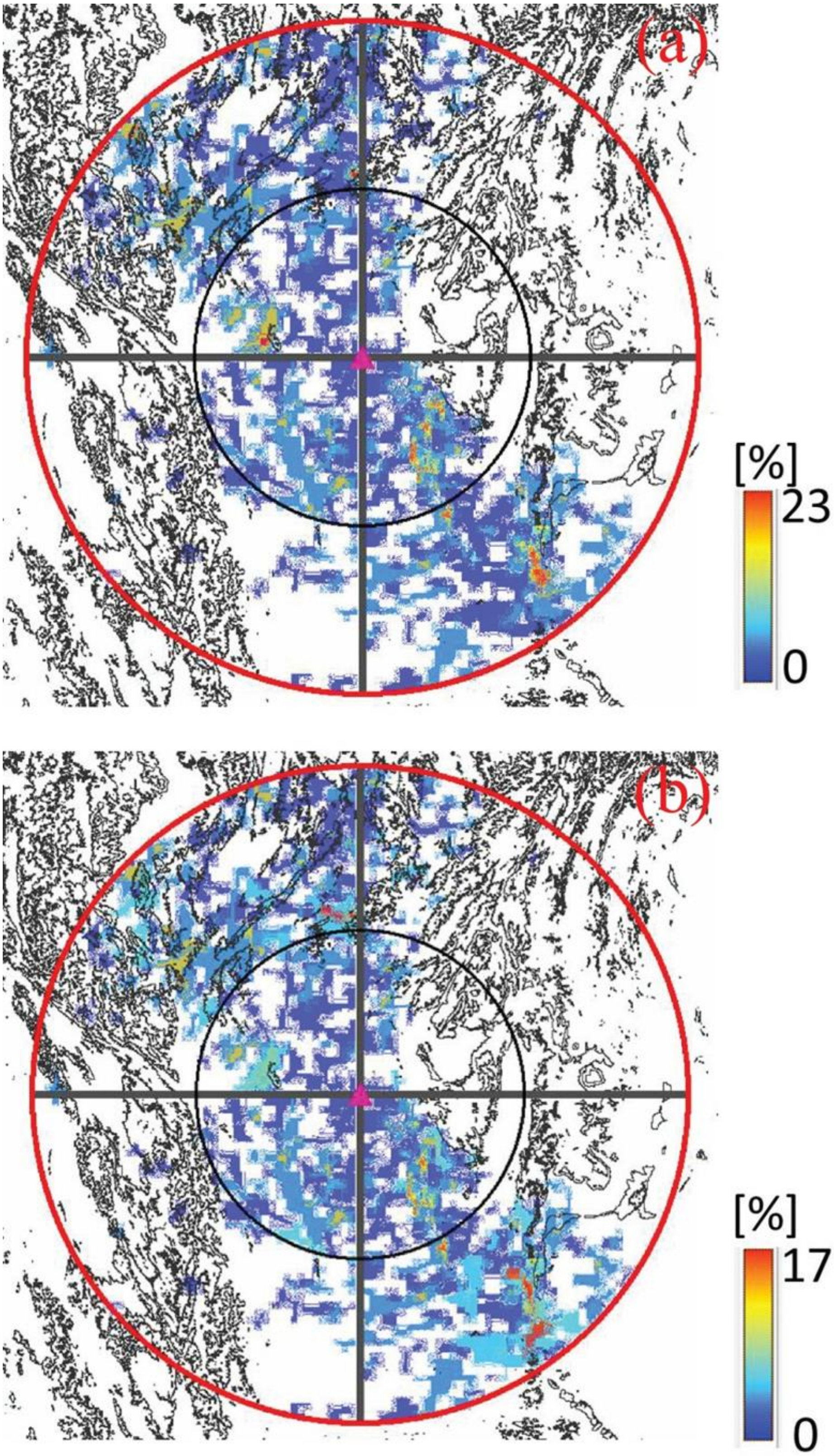

Figure 10: spatial distribution of convective storm frequency occurrence (a) composite of convective storm for 26 July 2017 (b) composite of the highest frequency of area average hour at 23, 12, 04 UTC

Spatial analysis of frequency occurrence for the storm can demonstrate the locations of severe convective storm occurrences as shown in Figure 10. The spatial pattern of convective cloud are located in both northwest and southeast of radar station ranging from mountainous areas to flood plain of Chao Phraya river basin. The high frequency of convective occurrence has been observed over the windward slope of mountain as shown in the composite map of 24-29 Jul 2017 especially on 26 Jul 2017. Composite of spatial convective cloud for the highest peak time of storm area occurs in the location of high frequency in the windward side as shown in Figure 10 (a) and Figure 10 (b). The Mae pool in Uttraradit province, north of the Phitsanulok radar station, where had historical suffered from landslide and flashflood, has shown frequency of convective storms at 17% during the storm period. In 2006, Asian Disaster Preparedness Center (ADPC) had observed flashflood/landslide damaging area over the northern region of Phitsanulok radar coverage in Uttaradit and Sukhothai provinces, after low pressure causing by severe tropical storm named Chanchu during 21-23 May 2006. The unusual rainfall intensity induced by low pressure causing from the severe storm Chanchu in early monsoon had largely affected the observed areas by destabilizing the slope over the risky area. The inappropriate landuse over high slope area in risky area had also been observed. ADPC suggested to have the monitoring the evolution of low pressure during dissipation of the tropical storm to issue some early warning over risky area that could decrease the damage from the flashflood and landslide. Therefore, the extracted radar information as convective region is one of the useful information during monsoon season in Thailand to monitor hydro-meteorological disasters especially for risky area. Moreover, to predict the inland decay of storms, understanding decaying typhoon characteristics is needed over the mid of ICP after the landfalls of Typhoon by using both observations and models. Not only rainfall induced by the decaying Typhoon, but also the producing wind during the Typhoon events are also needed to be elucidated. There is a model for predicting the decay of tropical cyclone winds after landfall that had been developed by Kaplan and DeMaria (1995). The model is developed a simple empirical model based on the least squares fit of an exponential decay equation to the NHC best-track 1-min maximum sustained surface wind estimates for all tropical storms and hurricanes that caused landfall in the south of 37°N United States for the period of 1967–93. The model shows that the maximum winds inland are a function of the maximum winds at landfall and the time after landfall. It can estimate the maximum inland penetration of winds of a given speed, where the storm’s landfall intensity and speed of motion are known. The radial velocity measured by Doppler radar is also needed to analyze because it can be used to validate the wind pattern from mesoscale numerical model such as the study of decaying Typhoon Lekima in 2007 done by Satomura et al., (2013).

5. Conclusion

The tropical storm named Sonca has been analyzed to find the spatio-temproal pattern over the Phitsanulok radar coverage area, in the middle of Thailand. The storm occurred over the study area during 24-29 July 2017 causing the large rainfall amount over the study area. The radar reflectivity from images operating by Thai Meteorological Department (TMD) has been downloaded through website of the Hydro and Agro Informatics Institute. The radar images at frequency of once per hour have been extracted by the developed method. The extracted reflectivity has been processed to detect convective cloud regions. Then, the spatio-temporal analysis of detected convective cloud has been done. The method and analysis have been developed using Python script and OpenCV, Computer Vision package to process image data. The developed method is practical to apply in reanalysis of storm in archiving images to understand the characteristics and mechanism of convective cloud which is the significant part to induce the disaster events such as flash flood and landslide over the middle of Thailand. In the spatio-temporal analysis of storm, it discovered the high frequency occurrence of the storm over the windward slope of mountain. The result of beam blockage analysis using Wradlib library has shown the east side of Phitsanulok radar severely suffering from terrain blocking the propagating beam. The usage of multiple radars to monitor over risky area is needed to overcome the beam blockage by terrain problem. The further study should be included the analysis of stratiform cloud to compare with the convective clouds. In addition, the atmospheric circulation before and during the storm events are needed to be investigate to understand the atmospheric circulation and structures of the event.

Acknowledgements

This research was supported by National Research Council of Thailand (NRCT) through the Naresuan University R2561B062 and R2561B063. We are really appreciated to “Advancing Co-design of Integrated Strategies with Adaptation to Climate Change in Thailand (ADAP-T)” supported by the

Science and Technology Research Partnership for Sustainable Development (SATREPS), JST-JICA for providing research fund to support the project. Special thanks to the Thai Meteorological Department and Hydro and Agro Informatics Institute for providing free downloadable radar reflectivity images. In addition, we gratefully thank to developer of OpenCV and Wradlib libraries for providing source codes used in Python script to be adapted in the processing of radar reflectivity images.

References

Asian Disaster Preparedness Center, 2006, Rapid Assessment: Flashflood and Landslide Disaster in the Provinces of Uttaradit and Sukhothai, Northern Thailand, May 2006, *Urban Disaster Risk Management*.

Austin, P. M. and Houze, Jr., R. A., 1970, Analysis of Mesoscale Precipitation Areas. *Proceedings, 14th Conference on Radar Meteorology*, *Boston, American Meteorological Society*, 329-334. Abstract in Bull. *American Meteor Society*, 51, 80.

Austin, P. M. and Houze, Jr., R. A., 1972, Analysis of the Structure of Precipitation Patterns in New England. *Journal of Applied Meteorology*, Vol. 11, 926–935.

Bangkok Post., 2017, North Suffers Effects of storm 'Sonca'. Available at: https://www.bangkokpost.com/news/general/1294527/north-suffers-effects-of-storm-sonca. [Accessed 17 Jul. 2018].

Biggerstaff, M. I. and Listemaa, S., 2000, An Improved Scheme for Convective/Stratiform Echo Classification using Radar Reflectivity, *Journal of Applied Meteorology*, Vol. 39, 2129–2150.

Carbone, R. E. and Tuttle, J. D., 2008, Rainfall Occurrence in the U.S. Warm Season: the Diurnal Cycle. *Journal of Climate*, Vol. 21, 4132-4146.

Duda, R. O. and Hart, P. E., 1972, Use of the Hough Transformation to Detect Lines and Curves in Pictures. *Communications of the ACM*, Vol. 15, 11-15.

Fitzgibbon, A. W. and Fisher, R. B., 1995, A Buyer's Guide to Conic Fitting. Proc.5th *British Machine Vision Conference*, Birmingham, 513-522.

He, Z., Zhang, Q. and Sun, J., 2016, The Contribution of Mesoscale Convective Systems to Intense Hourly Precipitation Events during the Warm Seasons over Central East China. *Advances in Atmospheric Sciences*, Vol. 33, 1233-1239.

Heistermann, M., Jacobi, S. and Pfaff, T., 2013, Technical Note: An Open Source Library for Processing Weather Radar Data (wradlib). *Hydrology and Earth System Sciences*, Vol. 17, 863-871.

Houze, Jr., R. A., 1973, A climatological study of vertical transports by cumulus-scale convection. *Journal of the Atmospheric Sciences*, 30, 1112–1123.

Houze, Jr., R. A., 2004, Mesoscale Convective Systems. *Reviews of Geophysics*, Vol. 42, 10.1029/2004RG000150, 43.

Kaplan, J. and DeMaria, M., 1995, A Simple Empirical Model for Predicting the Decay of Tropical Cyclone Winds After Landfall. *Journal of Applied Meteorology*, Vol. 34, 2499-2512.

Lang, T. J., Ahijevych, D. A., Nesbitt S. W. and Carbone, R. E., 2007, Radar-Observed Characteristics of Precipitating Systems During NAME 2004. *Journal of Climate*, Vol. 20, 1713-1733.

Mahavik, N., T. Satomura, S., Shige, B., Sysouphanthavong, S., Phonevilay, Wakabayashi, M. and Baimoung, S., 2014, Rainfall Pattern over the Middle of Indochina Peninsula During 2009–2010 Summer Monsoon. *Hydrological Research Letters*, Vol. 8, 57-63.

Nesbitt, S. W., Cifelli, R. and Rutledge, S. A., 2006, Storm Morphology and Rainfall Characteristics of TRMM Precipitation Features. *Monthly Weather Review*, Vol. 134, 2702-2721.

Rigo, T. and Llasat, M. C., 2004, A Methodology for the Classification of Convective Structures Using Meteorological Radar: Application to Heavy Rainfall Events on the Mediterranean coast of the Iberian Peninsula. *Natural Hazards and Earth System Sciences*, Vol. 4, 59-68.

Rabus, B., Eineder M., Roth A. and Bamler R., 2003, The shuttle radar topography mission - a new class of digital elevation models acquired by space borne radar. *Journal of Photogrammetry and Remote Sensing*, Vol. 57, 241-262.

Rigo, T. and Llasat, M. C., 2005, Radar analysis of the life cycle of Mesoscale Convective Systems during the 10 June 2000 event. *Natural Hazards and Earth System Sciences*, Vol. 5, 959-970.

Rigo, T. and Llasat, M. C., 2007, Analysis of Mesoscale Convective Systems in Catalonia Using Meteorological Radar for the Period 1996–2000. *Atmospheric Research*, Vol. 83(2-4), 458-472.

Rinehart, R. E., 1999, Radar for Meteorologists 3rd ed, Rinehart publication, P.O.Box6124, Grand Forks, ND 58206-6124, USA, 428.

Satomura, T., Yamamoto, K., Sysouphanthavong, B. and Phonevilay, S., 2011, Diurnal Variation of Radar Echo Area in the Middle of Indochina. *Journal of the Meteorological Society of Japan*, Vol. 89a, 299-305.

Satomura, T., Katsumata, M., Mori, S., Yokoi, S., Matsumoto, J., Ogino, S. and Kamimera, Y., 2013, To Understand Typhoons' Behavior Over Indochina. *Journal of Disaster Research*, Vol. 8, 153-154.

Schumacher, S. R. and Johnson, R. H., 2006, Characteristics of U.S. Extreme Rain Events during 1999–2003. *Weather and Forecasting*, Vol. 21, 69-85.

Steiner, M., Houze, Jr., R. A. and Yuter, S. E., 1995, Climatological Characterization of Three-Dimensional Storm Structure from Operational Radar and Rain Gauge Data. *Journal of Applied meteorology*, Vol. 34, 1978-2007.